Separation and Purification Technology 252 (2020) 117450

Contents lists available at ScienceDirect

Separation and Purification Technology

journal homepage: www.elsevier.com/locate/seppur

The development of reaction kinetics for CO_2 absorption into novel solvent systems: Frustrated Lewis pairs (FLPs)

Ozge Yuksel Orhan[a,*], Neslisah Cihan[a], Volkan Sahin[b], Abdulkerim Karabakan[b], Erdogan Alper[a]

[a] Hacettepe University, Department of Chemical Engineering, Beytepe, Ankara 06800, Turkey
[b] Hacettepe University, Department of Chemistry, Beytepe, Ankara 06800, Turkey

ARTICLE INFO

Keywords:
$B(C_6F_5)_2Cl$
Carbon dioxide capture
Frustrated Lewis pairs
Stopped-flow
tBu_3P

ABSTRACT

Frustrated Lewis Pairs (FLPs) comprising sterically hindered Lewis acids and bases were developed and kinetic parameters for the homogenous reaction between CO_2 and FLP dissolved in bromobenzene were obtained by using the stopped-flow method for the first time in the scope of this work. As a sterically hindered Lewis acid chlorobis(pentafluorophenyl)borane, $B(C_6F_5)_2Cl$ and as a sterically hindered Lewis base tri-*tert*-butylphosphine, tBu_3P were analyzed. Experiments were performed by varying FLP concentration in bromobenzene medium over the range of 0.02–0.035 M and for a temperature range of 298–313 K. Modified termolecular reaction mechanism was used to analyse the experimental kinetic data. Then, the relatively low reaction rate of FLP: bromobenzene system was enhanced significantly by blending constant amounts of promoters, such as amino ethyl piperazine (AEPZ), carbonic anhydrase (CA) and 1-ethyl-3-methyl imidazolium bis (trifluoromethyl sulfonyl) imide ([emim][Tf_2N]). The intrinsic reaction rates of promoted solvents were measured in a stopped-flow technique over a temperature range of 293–323 K. The empirical power law reaction orders with respect to FLP concentration were found to be between 1.0 and 2.0 at various temperatures. Additionally, at these operating conditions, the promoting effects of AEPZ, CA, and [emim][Tf_2N] results in a higher reaction rate and lower activation energy values.

1. Introduction

Carbon dioxide (CO_2), which is especially exhausted at high levels at thermal power plants, has a significant impact on global warming and climate change among greenhouse gases (GHGs) [1]. Over the last 120 years, due to the increase of anthropogenic CO_2 emissions, the concentration of CO_2 in the atmosphere has increased from 280 ppm to 390 ppm and in the mid of 21st century, the amount of CO_2 in the atmosphere is expected to double [2]. The uncontrolled emissions of carbon dioxide to the atmosphere are an international issue because of the greenhouse gas effect, and separation of it from other non-acidic gases and harmless storage ("CO_2 sequestration") is on the world agenda and applications have already begun [3].

Although the CO_2 level in the atmosphere causes the global warming problem, fossil fuels are still the most widely used energy resources due to their high energy capacity and availability. Therefore, CO_2 capture and storage (CCS) has become increasingly important in recent years [4]. The main purpose of these studies is to improve absorption liquids and the design of processes [5]. It is generally accepted that the most convenient method is chemical absorption of CO_2 into aqueous amine solutions (monoethanolamine (MEA), diethanolamine (DEA), N-methyl diethanolamine (MDEA), etc.) and then regeneration of solution with desorption [6,7]. The solvent chosen for carbon dioxide absorption should have low vapour pressure, viscosity, and corrosiveness, and also the selected solvent system should have high CO_2 selective solubility, absorption rate and the CO_2 loading capacity [8]. In addition, it should have -relatively- easy regeneration [9]. However, conventional aqueous amine-based solvents have high corrosiveness and owing to the large specific heat capacity and vaporization enthalpy of water, the high amount of sensible heat and latent heat required for heating and vaporization of water result in high energy consumption [10–13]. For these reasons, the development of novel solvent formulations -especially organic- has gained importance. Non-aqueous absorbents have shown promising prospects due to their high energy saving potential, low degradation, and low corrosiveness [14]. A novel approach to capture CO_2 is the use of frustrated Lewis pairs (FLPs). Lewis pairs that have steric hindrance property show low reactivity to neutralization reactions (Fig. 1). By adding the small molecules such as

* Corresponding author.
E-mail addresses: oyuksel@hacettepe.edu.tr (O. Yuksel Orhan), neslisahcihan@hacettepe.edu.tr (N. Cihan), volkansahin@hacettepe.edu.tr (V. Sahin), kerimk@hacettepe.edu.tr (A. Karabakan), ealper@hacettepe.edu.tr (E. Alper).

https://doi.org/10.1016/j.seppur.2020.117450
Received 24 May 2020; Received in revised form 17 July 2020; Accepted 20 July 2020
Available online 26 July 2020
1383-5866/

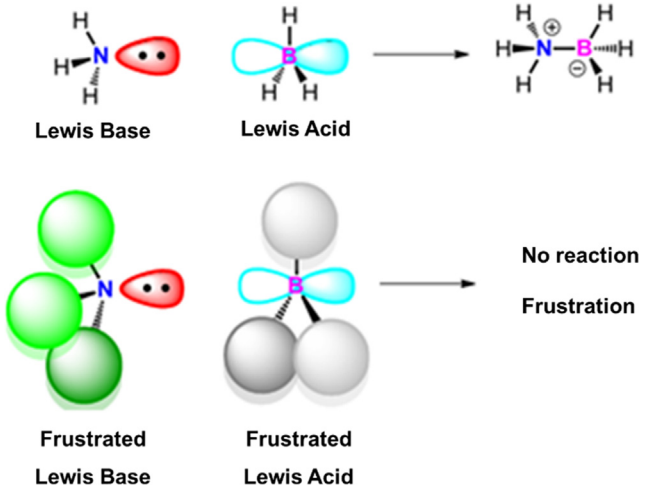

Fig. 1. Lewis acid–base interactions [15].

H_2, CO, CO_2, N_2O can become more reactive to generate opportunities unstable by-products [15]. Stephen and his co-workers pointed out the idea that the FLPs could also be a new and effective solvent system for post- combustion CO_2 capture [16–18]. The thermodynamic parameters, ΔG°, ΔH° and ΔS° of the FLP, $tBu_3P/B(C_6F_5)_2Cl$ were reported by Stephan and coworkers who described intramolecular and intermolecular B/P-based FLPs for CO_2 capture and also H_2 activation [16,17,19–21]. They also examined CO_2 insertions into combinations of sterically demanding phosphines and boranes and performed reaction pathways for the exchange chemistry of B/P-based FLP-CO_2 complexes [22]. These publications were inspired to design this study. Liu et al. reported theoretical studies to investigate the complete reaction pathway for CO_2 capture by the $tBu_3P/B(C_6F_5)_3$ [23]. They performed density functional theory (DFT) calculations and proposed that Lewis acid plays a more important role than the Lewis base.

As a sterically hindered Lewis acid chlorobis(pentafluorophenyl) borane, $B(C_6F_5)_2Cl$ and as a sterically hindered Lewis base tri-*tert*-butylphosphine, tBu_3P, were selected in this study. The chemical structures of selected Lewis acid and Lewis base are presented in Fig. 2. The kinetic parameters for the homogenous reaction between CO_2 and FLP ($tBu_3PB(C_6F_5)_2Cl$) dissolved in bromobenzene were obtained at various concentrations and temperatures by the using stopped-flow method.

Furthermore, it is intended to promote or enhance the low reaction rate constants of CO_2–FLP: bromobenzene by blending small amounts of selected activators. Firstly, the enzymatic approach was proposed to find an activator. Carbonic anhydrase (CA) is very efficient and one of the fastest biocatalyst known and plays a critical role in catalyzing the reversible reactions of CO_2 and water to bicarbonate (HCO_3^-) [24,25]. It also helps to reduce the activation energy of (bio)chemical reactions [26]. Versteeg et al. studied on CO_2 absorption-desorption performance of aqueous amine systems in the presence and absence of CA enzyme, they observed that the rate of absorption in the enzyme medium has increased and the energy is used more efficiently [27,28]. Deckwer and

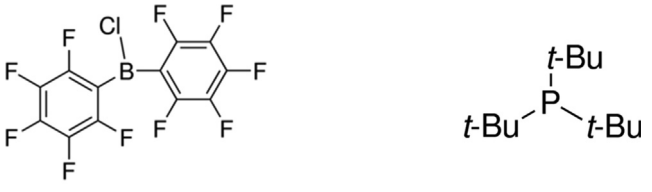

$B(C_6F_5)_2Cl$ **tBu_3P**

Fig. 2. Chemical structure of Lewis acid and Lewis base.

Alper examined the effect of CA buffer on CO_2 absorption they obtained favorable results for absorption kinetics of promoted amine solvents [29]. Based on the catalytic effect of CA on the reaction rate between CO_2 and amine systems, the use of CA to increase the low reaction rates of frustrated Lewis pair was investigated in detail for the first time.

Piperazine (PZ) and its derivatives are known to have high absorption capacity, fast reaction rate, and high resistance to thermal and oxidative degradation with the reaction CO_2 [30,31]. They become more and more popular due to the mentioned properties and have been also studied previously by our group [32–35]. PZ is a secondary amine with a ring-shaped structure and two amino groups. Due to the ring structure, it is estimated that CO_2 can approach hydrogen atom attached to the amino site with less steric hindrance. Other cyclic structure PZ derivative diamines, such as 1-(2-aminoethyl) piperazine (AEPZ) and 1-(2-hydroxyethyl) piperazine (NHEPZ) can be used as activators [35–37]. In this study, AEPZ was selected as an activator alternative owing to its high reaction rate and high solubility [35,38].

In another part of the study, a detailed literature search was performed to enhance the low reaction rates of FLP: bromobenzene system with CO_2 and as a radical approach, the idea of ionic liquid (IL) has been proposed inspired by Dyson et al. publication [39]. Ionic liquids are composed of various small anions and big heterocyclic organic cations and that can remain in the liquid form in the wide temperature range [40]. They are becoming increasingly popular with its unique properties such as high thermal stability, favourable CO_2 solubility, tunable physicochemical properties, and negligible vapour pressure [41]. Experimental and theoretical studies have shown that CO_2 is more soluble in certain imidazolium-based ILs [42]. The alkyl-side chain length of the imidazole-based cation also affects the solubility of CO_2 in the ionic liquid. Anion has a stronger effect on gas solubility than cation [43]. In this study, an imidazolium-based ionic liquid 1-ethyl-3-methylimidazolium ([emim] $[Tf_2N]$) was selected, due to its appropriate properties, such as low viscosity and the high CO_2 solubility [42].

As a result, although there have been theoretical studies and thermodynamic calculations for the reversible reactions between FLPs and CO_2, there is no reaction kinetics data related to FLP-CO_2 species in the literature [17,22]. In the scope of this paper, the reaction kinetics of the FLP system with CO_2 were examined in detail for the first time. The novelty of this work is the calculation of observed pseudo-first-order reaction rate constants (k_o, s^{-1}), the order of the reaction, the forward reaction rate constants and activation energies of CO_2–$tBu_3P/B(C_6F_5)_2Cl$ system in the absence and presence of promoters (CA, AEPZ, [emim][Tf_2N]) using the stopped-flow approach.

2. Theoretical

Reaction kinetics of the FLP system, consisting of a combination of sterically hindered acids and bases, with CO_2 were examined in detail for the first time. First, frustrated Lewis pair "$tBu_3PB(C_6F_5)_2Cl$" was formed and the reaction kinetics with CO_2 in bromobenzene was investigated experimentally by the "stopped-flow" method. The reaction mechanism of the carbon dioxide-sterically hindered Lewis pairs is as shown in Eq. (2.1) [22].

$$ClB(C_6F_5)_2 + tBu_3P \underset{-CO_2}{\overset{CO_2}{\underset{80\,^\circ C}{\rightleftharpoons}}} (C_6F_5)_2\overset{Cl}{\overset{|}{B}}-\overset{-}{O}-\overset{O}{\overset{\|}{C}}-P^+(tBu)_3 \quad (2.1)$$

Amine reactions will be mentioned briefly, considering that there may be a similarity with FLP systems. The termolecular reaction mechanism, zwitterion mechanism, and base-catalyzed hydration mechanism are applicable reaction mechanisms to explain the reaction between CO_2 and amine systems [44–46].

The termolecular reaction mechanism has been proposed by Crooks

and Donnellan mooted that an amine molecule reacts with both CO_2 and base molecule by forming weakly-bounded intermediate products in a single step [45]. Eq. (2.2) shows a general expression of the termolecular reaction mechanism for a primary amine.

$$CO_2 + RNH_2 \cdots\cdots\cdots\cdots B \rightleftarrows RNHCOO^- \cdots\cdots\cdots\cdots BH^+ \quad (2.2)$$

Here B denotes the base and RNH_2 is the amine. Under pseudo first-order conditions (where the solvent would be in excess), the observed forward reaction rate can be expressed as in Eq. (2.3).

$$r_{obs} = k_o[CO_2] \quad (2.3)$$

The modified termolecular reaction mechanism can be adapted to the mechanism of CO_2 into the FLP system, consisting of a combination of sterically hindered Lewis acids and Lewis bases, dissolved in bromobenzene (Br) as shown in Eq. (2.4).

$$r_{obs} = k_{FLP}[FLP][FLP] + k_{Br}[Br][FLP]\,[CO_2] \quad (2.4)$$

The observed reaction rate constant (k_o) can be expressed by Eq. (2.5).

$$k_o = \{k_{FLP}[FLP] + k_{Br}[Br]\}\,[FLP] \quad (2.5)$$

It has been reported that the reaction mechanism is suitable to describe the degree of fractional reaction order can change between 1 and 2 relative to the reactant [34,47,48].

Since bromobenzene concentration is assumed to be in excess for the pseudo first-order conditions, Br can be considered constant and a new rate constant, k, can be defined by $k = k_{Br}[Br]$.

$$k_o = k_{FLP}[FLP] + k[FLP] \quad (2.6)$$

Also if the bromobenzene is the dominant base, the system exhibits a first-order reaction and Eq. (2.6) reduces to Eq. (2.7).

$$k_o = k[FLP] \quad (2.7)$$

When CA is blended as a promoter, Eq. (2.5) can be modified as:

$$k_o = k_{FLP}[FLP][FLP] + k_{Br}[Br][FLP] + k'_{Br}[Br][CA] + k_{FLP-CA}[FLP]\,[CA] \quad (2.8)$$

The principal difference between Eq. (2.8) and the termolecular mechanism as proposed by Crooks and Donnellan is that while they consider only an amine as the third molecule, in modified termolecular mechanism solvent (bromobenzene) is also subsumed as well as the blended FLP systems as proposed previously by Gordesli and Alper [33] and Ozturk et al. [47]. Similarly, considering that the bromobenzene is in excess and nearly at a constant concentration, $k = k_{Br}[Br]$ and $k^* = k'_{Br}[Br]$ can be presumed to be constant so Eq. (2.9) is obtained.

$$k_o = k_{FLP}[FLP][FLP] + k[FLP] + k*[CA] + k_{FLP-CA}[FLP][CA] \quad (2.9)$$

Under experimental conditions, [CA] is kept constant and [FLP] is varied. When [CA] is kept constant at $[CA]_0$, the following equations are obtained:

$$k_o = k[FLP] + k_{FLP}[FLP][FLP] + k*[CA]_0 + k_{CA-FLP}[CA]_0[FLP] \quad (2.10)$$

which reduces to:

$$k_o = k_1 + k_2[FLP] + k_{FLP}[FLP][FLP] \quad (2.11)$$

where, $k_1 = k^*\,[CA]_0$ and $k_2 = k + k_{CA\text{-}FLP}[CA]_0$ are constants.

Other recommended approach to enhance the low reaction rate constants of FLP-CO_2 reactions is the addition of amine promoters, such as AEPZ and [emim][Tf_2N].

The following equation is valid for the pseudo first-order reaction rate constant according to the modified termolecular reaction mechanism of hybrid systems consisted of the blends of ionic liquid ([emim][Tf_2N]) or piperazine derivative cyclic amine (AEPZ) with FLP in bromobenzene medium:

$$k_o = k_{Br}[Br][P] + k'_{Br}[Br][FLP] + k_P[P][P] + k_{FLP}[FLP]\,[FLP] + k_{FLP-P}[FLP][P] \quad (2.12)$$

Here P refers to [emim][Tf_2N]) or AEPZ.

Considering that bromobenzene is in excess and nearly at a constant concentration, $k = k_{Br}[Br]$ and $k^* = k'_{Br}[Br]$ can be assumed to be constant so Eq. (2.13) is obtained.

$$k_o = (k + k_P[P])[P] + (k* + k_{FLP}[FLP])[FLP] + k_{FLP-P}[P][FLP] \quad (2.13)$$

Under experimental conditions, [P] is kept constant and [FLP] is varied. When [P] is kept constant at $[P]_0$, the following equations are obtained:

$$k_o = (k + k_P[P]_0)[P]_0 + (k* + k_{FLP}[FLP])[FLP] + k_{FLP-P}[P]_0[FLP] \quad (2.14)$$

which reduces to:

$$k_o = k_4 + k_3[FLP] + k_{FLP}[FLP][FLP] \quad (2.15)$$

where, $k_4 = (k + k_P\,[P]_0)[P]_0$ and $k_3 = k^* + k_{FLP\text{-}P}[P]_0$ are constants.

Since bromobenzene is assumed to be in excess for the pseudo first-order conditions and the promoter concentration [P] is kept constant under experimental conditions, the reaction order with respect to FLP will result from Eq. (2.16).

$$k_o = k[FLP] \quad (2.16)$$

According to this equation, if k_o (s^{-1}) is plotted according to the FLP concentration, the rate constant, k (m^3/kmol·s) is obtained from the slope by linear regression.

If the FLP and bromobenzene are comparably dominant bases, fractional reaction order with respect to FLP exists and the reaction degree can change between 1 and 2. The observed reaction rate constant (k_o) can be defined by Eq. (2.17).

$$k_o = k[FLP] + k_{FLP}[FLP]^2 \quad (2.17)$$

If k_o (s^{-1}) is plotted according to the FLP concentration, the rate constants, k (m^3/kmol·s), and k_{FLP} (m^6/$kmol^2$·s) are obtained from the slope by linear regression.

If FLP is the dominant base, then the effect of bromobenzene on the reaction is negligible beside the FLP and system exhibits second order with respect to FLP. The observed reaction rate constant (k_o) can be defined by Eq. (2.18).

$$k_o = k_{FLP}[FLP]^2 \quad (2.18)$$

According to this equation, if k_o (s^{-1}) is plotted according to the square of FLP concentration, the rate constant, k_{FLP} (m^6/$kmol^2$·s) is obtained from the slope by linear regression.

3. Materials and methods

3.1. Materials

tBu_3P: Tri-Tert-Butylphosphine, 98% (CAS no. 13716-12-6) with a purity of 98% was purchased from Sigma-Aldrich. Carbon dioxide gas was obtained by Linde (Germany) with 99.99% purity. Bromobenzene (CAS no. 108-86-1) with a purity of 99%, AEPZ: 1-(2-Aminoethyl)piperazine (CAS no. 140-31-8) with a purity of 99%, ([emim][Tf_2N]): 1-Ethyl-3-methylimidazolium bis(trifluoromethylsulfonyl)imide (CAS no. 174899-82-2) for synthesis and CA: carbonic anhydrase (CAS no. 9001-03-0) from bovine erythrocytes were supplied from Sigma-Aldrich. B$(C_6F_5)_2Cl$: chlorobis(pentafluorophenyl)borane was synthesized as described in Section 3.2. Bromopentafluorobenzene, (CAS no. 344-04-7) with a purity of 99%, magnesium powder (CAS no. 7439-95-4) with a purity of ≥99%, diethyl ether (CAS no. 60-29-7) with a purity of ≥99.5%, and boron trichloride solution 1.0 M in heptane (CAS no. 10294-34-5) were purchased from Sigma-Aldrich and used for the

synthesis of $B(C_6F_5)_2Cl$.

3.2. Synthesis of chloro-bis(pentafluorophenyl)borane

0.292 g (0.012 mol) magnesium and 10 mL dehydrated diethyl ether are mixed inside the three-necked glass flask that is bounded to condenser and accompanied with nitrogen gas switch system. 2.469 g (0.01 mol) bromopentafluorobenzene solution inside 10 mL dehydrated diethyl ether is added on magnesium suspension. The Grignard reactive is constituted by boiling that mixture under the condenser for 30 min. 3.7 g (0.005 mol) borontrichloride solution is added on another three-necked glass flask that is bounded to distillation funnel. This glass flask is submerged into water and mixed by magnetic stirrer while Grignard reactive (C_6F_5-MgBr) is added to flask drop by drop. When the adding process is over, the flask is taken from the ice bath and stirred under the condenser during 24 h. The obtained mixture is diluted in 20 mL diethyl ether, quenched with 1 M ammonium chloride. The product is precipitated by adding petroleum ether and separated by filtration at 50 °C. The obtained powder product in 76% crude yield (1.45 g, 3.8 mmol) was characterized as chloro-bis(pentafluorophenyl)borane by MALDI-TOF MS. No impurities were found in the analysis conditions performed.

3.3. Characterization of chloro-bis(pentafluorophenyl)borane

Fig. 3 shows the molecule structure and MALDI-TOF-MS (Matrix Assisted Laser Desorption/Ionization-Time of Flight-Mass Spectrometer) analyzes the results of chloro-bis(pentafluorophenyl)borane Lewis acid that is synthesized by Grignard reaction. The ion peak of the molecules obtained by electron ejection from molecule 1 (*m/z*: 379.9) is the most severe signal in the spectrum. The natural abundances of two isotopes of chlorine element with the mass of 34.97 and 36.50 akb are 75.53 and 24.77% respectively. The natural abundances of two isotopes of carbon element with the mass of 12 and 13 akb are 90 and 10% respectively. The ^{11}B and ^{10}B isotopes of boron element have natural abundancy of 80 and 20% while ^{19}F is the major isotope of fluorine element. The signal with mass value of 380.7 akb belongs to the molecules containing ^{13}C and $^{34.97}Cl$ isotopes and the signal of 381.3 akb ^{12}C and $^{36.53}Cl$ isotopes. The signal at 212.8 *m/z* belongs to fragmentation product that is obtained by de-linking of pentafluorophenyl group from chloro-bis(pentafluorophenyl)borane. Other signals that are seen in the spectrum belong to matrix which is used during analyzes. The mass spectrum shows that the products carry 1 chlorine and 2 pentafluorophenyl groups.

All mass spectra were performed using a Voyager-DE Pro MALDI-TOF mass spectrometer (Applied Biosystems, USA). Ionization and desorption of samples were obtained using the 337 nm from a pulsed nitrogen laser (Spectra Physics, USA) at ca. 10–7 Torr. For ion extraction, an acceleration potential of 25 kV was used in the source region [49].

3.4. Stopped-flow experiments

The reaction kinetics for the homogeneous reactions between dissolved CO_2 and FLP systems in the presence and absence of promoters (CA, AEPZ, [emim][Tf_2N]) were performed by using a stopped-flow equipment for concentration range from 0.02 M to 0.035 M over temperature range of 298–323 K. The stopped-flow instrument (model SF-61SX2, manufactured by Hi-Tech Scientific, UK) is designed for direct determination of the pseudo first-order kinetics data of a rapid reaction by measuring conductivity change during the reaction. The system consists of four major parts: the sample handling unit, conductivity detection cell, A/D converter unit and microprocessor unit. The entire flow circuit is thermostated and the temperature control is better than 0.1 K. Stopped-flow technique enables to determine pseudo first-order reaction rates usually ranged between about 0.01 and 2500 s^{-1}, the upper limit corresponding to the inverse of the mixing time which is close to 1 ms [42]. The run time of the experiments was varied from 0.05 to 0.1 s depending on the concentration and temperature. For each run, a freshly saturated CO_2 solution obtained by bubbling CO_2 gas through bromobenzene and FLP: bromobenzene solution were loaded in two separate syringes. Equal volumes (50 µl reagent from 5 mL sample syringes) of FLP: bromobenzene solution and CO_2 dissolved in bromobenzene were mixed rapidly in conductivity cell. For a typical measurement, the variation of ionic species concentrations is monitored by the change of conductance in the solution. An increasing signal of electrical conductivity is observed due to the formed ionic products at the beginning of the reaction and when the reaction reaches equilibrium, the signal tends to be stable. A (S) is the amplitude of the signal, k_0 the pseudo first-order kinetic constant (s^{-1}), t (s) is the time and Y_∞ (S) is the value of the conductance at the end of the observed reaction. Variation of conductance is then related to formation of products and to k_0 according Eq. (3.1) [50,51].

$$Y = -Aexp(-k_o t) + Y_\infty \quad (3.1)$$

To satisfy the pseudo first-order condition, reactant concentration was kept about 20 times to CO_2 concentration dissolved in bromobenzene. Each experimental set was repeated at least 8 times to obtain consistent pseudo first-order rate constants (k_o) at each temperature for

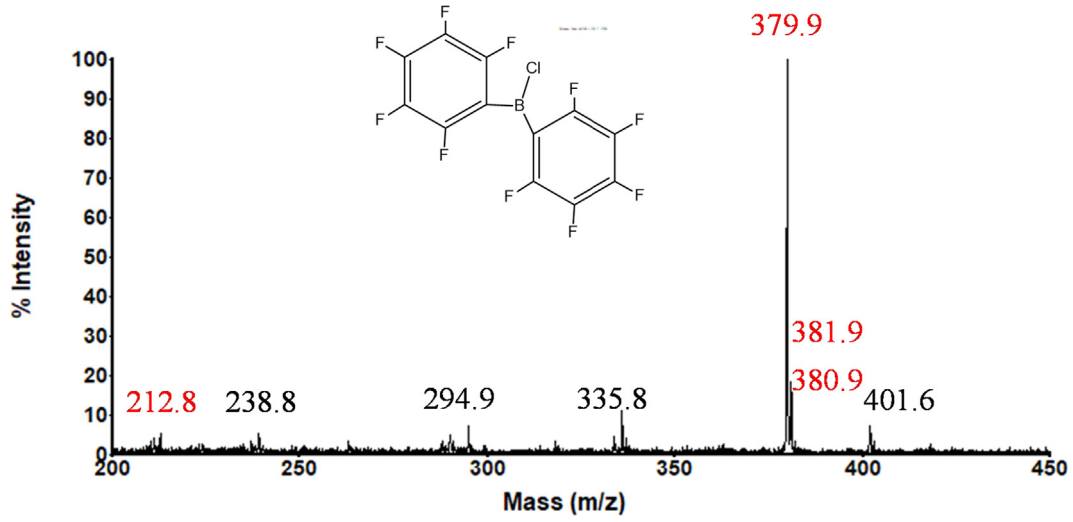

Fig. 3. MALDI-TOF MS spectrum for chloro-bis(pentafluorophenyl)borane.

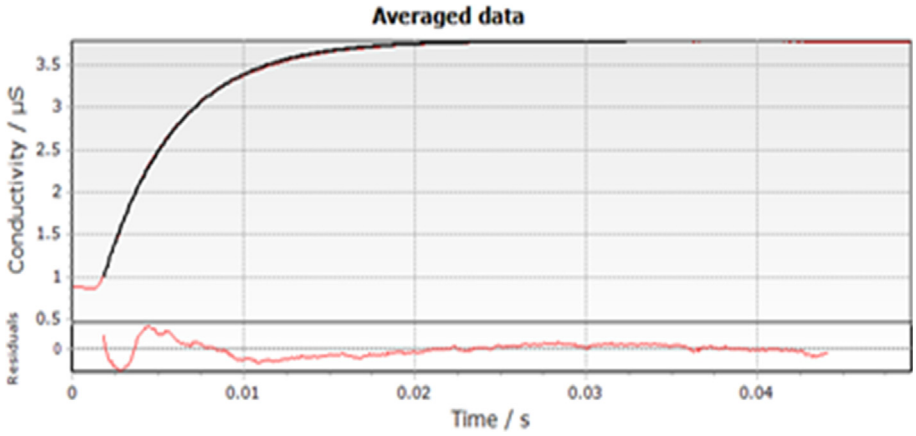

Fig. 4. Typical combined graph for 0.035 M FLP: bromobenzene system at 313 K.

all concentrations. The observed pseudo first-order rate constants (k_o) were obtained by a least square regression. Average k_o values can be detected for each experimental set by the equipment software. A typical graphical output is presented in Fig. 4 for 0.035 M FLP in bromobenzene system at 313 K. A detailed description of the stopped-flow apparatus and experimental procedure can be found elsewhere [42,47,52,53].

4. Results and discussion

4.1. Kinetic parameters

In this study, the FLP system consists of a mixture of a Lewis acid: B$(C_6F_5)_2$Cl and Lewis base: *t*Bu$_3$P dissolved in bromobenzene were developed. Intrinsic reaction rates were measured directly for a temperature range of 298–313 K. Experimentally obtained pseudo–first order reaction rate constants for CO_2-FLP: bromobenzene system at different concentrations and temperatures were given in Table 1.

Measured pseudo first-order reaction rate constants of the reaction between CO_2 and FLP: bromobenzene systems prepared at three different concentrations and four different temperatures.

To justify the validity of the termolecular mechanism, the natural logarithms of observed reaction rate constants versus FLP concentrations were plotted as shown in Fig. 5. Empirical power-law kinetics was fitted to lines in by using the least square method. The slopes of the fitted lines correspond to the order of the reaction. Order of the reactions with respect to FLP are determined as approximately 1.00 with regression values of R^2 = 0.98–0.99 that are in accordance with the modified termolecular reaction mechanism suggested in Eq. (2.7).

The forward reaction rate constants of CO_2-FLP: bromobenzene system were determined by fitting observed reaction rate constants versus FLP concentrations. As seen in Fig. 6, it is very satisfactorily compatible with the pseudo first-order plot.

As expected, k_o, values increase as both the FLP concentration and the temperature over 0.02–0.035 M and 298–313 K respectively. The forward reaction rate constants for CO_2-FLP: bromobenzene systems were summarised in Table 2.

Arrhenius plot according to Arrhenius equation (Eq. (4.1)) were used to obtain the activation energies of the reaction between CO_2 and FLP: bromobenzene systems.

Table 1
Observed pseudo–first order reaction rate constants for CO_2-FLP: bromobenzene system.

	k_o (s^{-1})		
[FLP]: bromobenzene (kmol/m^3)	0.02	0.027	0.035
298 K	1.0	1.4	1.8
303 K	1.6	2.4	2.8
308 K	3.2	4.9	5.9
313 K	6.0	8.9	10.5

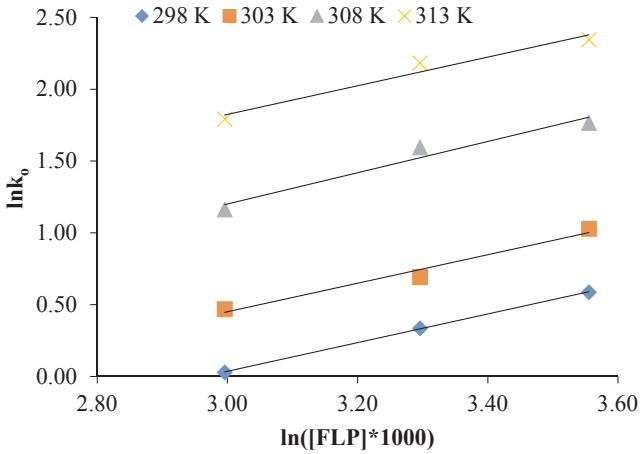

Fig. 5. Apparent reaction order plot for CO_2-FLP: bromobenzene system at various temperatures.

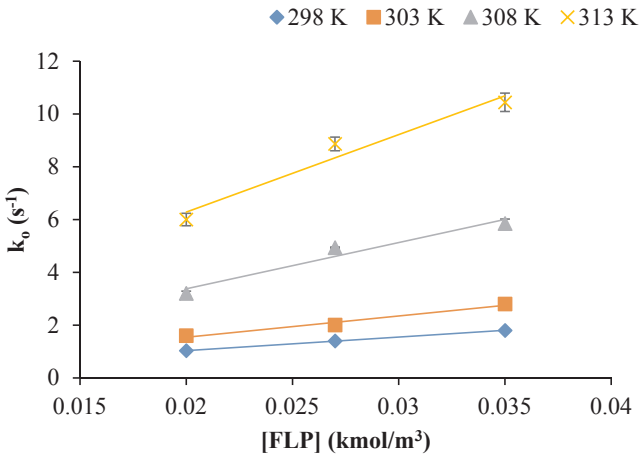

Fig. 6. Pseudo first-order rate constants as a function of FLP concentration for CO_2-FLP: bromobenzene system at various temperatures. All data are the average of at least eight replicate experiments, and error bars are the standard deviation of the mean.

Table 2
The forward reaction rate constants of the FLP: bromobenzene system at various temperatures.

Temperature (K)	298	303	308	313
k (m^3/kmol·s)	52	78	171	308

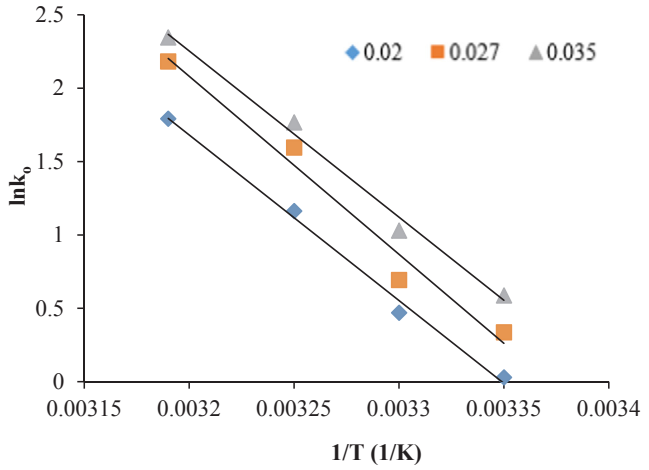

Fig. 7. Arrhenius plot for CO_2-FLP system in bromobenzene medium.

$$k = A\exp\left(-\frac{E_a}{RT}\right) \quad (4.1)$$

where A is the Arrhenius factor (m^3/mol s), and E_a is the activation energy (kJ/mol).

According to the Arrhenius plot (Fig. 7), the average activation energy of the FLP: bromobenzene systems was found around 96 kJ/mol.

The obtained forward reaction rate constant of CO_2 absorption into FLP: bromobenzene system was compared with some conventional aqueous amine solutions reported in literature. As primary amine MEA, secondary amines (DEA, MAE (methyl-aminoethanol), 1A2P (1-amino-2-propanol) and 3A1P (3-amino1-propanol)), and tertiary amines (MDEA, DMEA (N,N-dimethylethanolamine), DEEA (N,N-diethylethanolamine), 1DEA2P (1-diethylamino-2-propanol) and DEAB (4-diethylamino-2-butanol)) were selected and summarized in Table 3. Besides, the forward reaction rate constants of sterically hindered amine (AMP (2-amino-2-methyl-1-propanol)) and cyclic diamine PZ were presented. It can be seen that, the forward reaction rate constant of FLP: bromobenzene system is much lower than primary and secondary aqueous solutions but comparable with tertiary amines.

Due to the low reaction rate constants of FLP: bromobenzene system, it is intended to enhance the reaction rates with the addition of promoters. To accelerate the FLP-CO_2 reaction mechanism, constant amounts of CA enzyme, AEPZ and [emim][Tf_2N] were added to three different concentrations of FLP: bromobenzene system for a temperature range of 298 K–323 K. The reaction mechanisms and kinetics were analyzed experimentally by using stopped-flow conductimetry method and modelled according to a modified termolecular reaction mechanism.

Table 3
The FLP: bromobenzene reaction rate constant of CO_2 absorption into aqueous amine solutions at 298 K.

Amine	k (m^3/kmol s)	References
FLP: bromobenzene	52	This study
MEA	5939	[54]
DEA	412	[55]
MAE	5381	[50]
1A2P	4314	[56]
3A1P	7475	[56]
MDEA	6.71	[57]
DMEA	27.2	[58]
DEEA	79.8	[58]
1DEA2P	91.2	[58]
DEAB	429	[59]
AMP	473	[60]
PZ	65460	[61]

Table 4
Observed pseudo–first order reaction rate constants for CO_2- CA: FLP: bromobenzene system.

	k_o (s^{-1})		
CA: FLP: bromobenzene (kmol/m^3)	0.02	0.027	0.035
298 K	28	44	63
303 K	34	52	75
308 K	39	57	83
313 K	44	64	92
318 K	47	66	96
323 K	54	73	100

4.2. The reaction kinetics of CO_2 and FLP: bromobenzene system promoted by CA

Intrinsic reaction rates of blends of FLP: bromobenzene system with CA were measured directly in the stopped-flow apparatus for a temperature range of 298–323 K. For all experiments, the CA concentrations were kept constant at 100 g/m^3. The concentration of FLP: bromobenzene system was increased between 0.02 M and 0.035 M. Experimentally obtained pseudo–first order reaction rate constants for CO_2- CA: FLP: bromobenzene system at different concentrations and temperatures were given in Table 4.

The observed rate constants of the reaction between CO_2 and promoted systems with respect to FLP concentrations at various temperatures were plotted as seen in Fig. 8. The forward reaction rate constants of CO_2-CA: FLP: bromobenzene system were determined from the slopes of fitted lines with high regression values of $R^2 = 1$ and summarised in Table 5.

Since the FLP: bromobenzene concentrations are constant in the mixture and the same temperature was used as in Section 4.1, the increase in the k_o values can be conceived as the promoting effect of the addition of CA.

Natural logarithms of k_o values versus FLP concentrations were plotted at various temperatures as shown in Fig. 9. The reaction orders

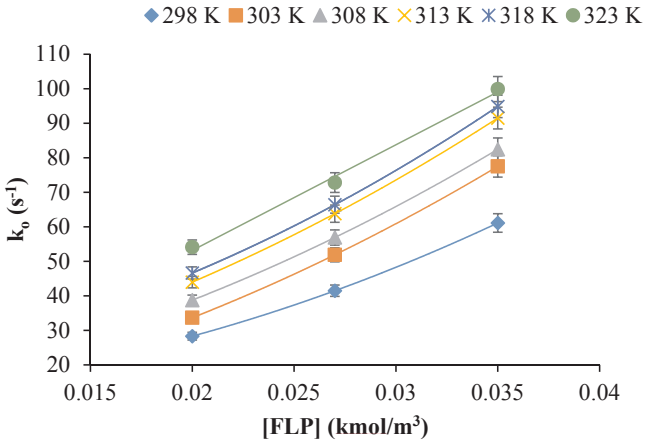

Fig. 8. Pseudo first-order rate constants as a function of FLP concentration for CO_2-CA: FLP: bromobenzene system at various temperatures. All data are the average of at least eight replicate experiments, and error bars are the standard deviation of the mean.

Table 5
The forward reaction rate constants of the CA: FLP: bromobenzene system at various temperatures.

T (K)	k_{FLP} ($m^6/kmol^2 \cdot s$)	k ($m^3/kmol \cdot s$)
298	22,947	937
303	27,671	1152
308	28,565	1352
313	29,747	1577
318	30,401	1661
323	–	2776

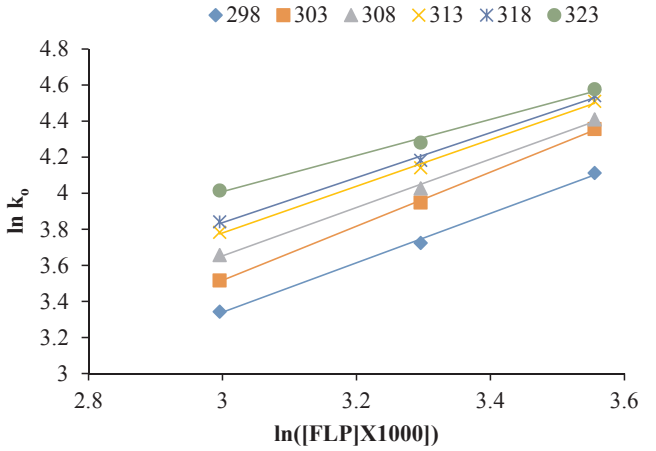

Fig. 9. Apparent reaction order plot for CO_2-CA: FLP: bromobenzene system at various temperatures.

of the CA: FLP: bromobenzene system were determined.

The slopes of fitted to lines harmonized to the reaction orders of the CA: FLP: bromobenzene system which are determined to be 1.4 at 298 K; 1.5 at 303 K; 1.3 at 308 K; 1.3 at 313 K; 1.3 at 318 K; 1.0 at 323 K with regression values of $R^2 = 0.99$.

Fig. 10 shows the Arrhenius plot for 100 g/m^3 CA promoted CO_2-FLP: bromobenzene system at 0.02 M, 0.027 M and 0.035 M, respectively. Arithmetic mean activation energy for the CO_2- CA: FLP: bromobenzene system was calculated as 17 kJ/mol by using the slopes of fitted lines.

4.3. The reaction kinetics of CO_2 and FLP: bromobenzene system promoted by AEPZ

Intrinsic reaction rates of blends of FLP: bromobenzene system with AEPZ were measured directly for a temperature range of 298–323 K. AEPZ concentrations were kept constant at 100 g/m^3 and the concentration of FLP: bromobenzene system were increased between

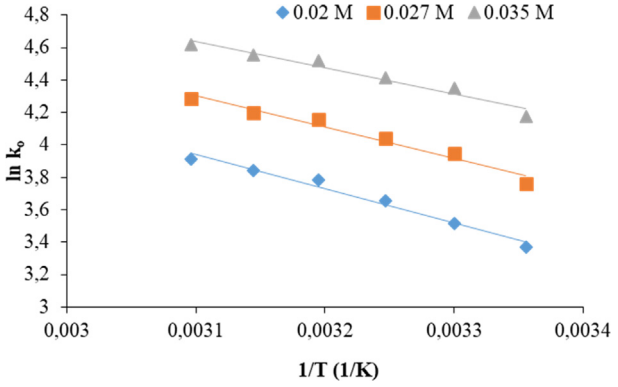

Fig. 10. Arrhenius plot for CO_2- CA: FLP system in bromobenzene medium.

Table 6
Observed pseudo–first order reaction rate constants for CO_2- AEPZ: FLP: bromobenzene system.

	k_o (s^{-1})		
AEPZ: FLP: bromobenzene ($kmol/m^3$)	0.02	0.027	0.035
298 K	33	50	71
303 K	37	55	77
308 K	42	59	84
313 K	44	64	90
318 K	50	70	100
323 K	58	75	102

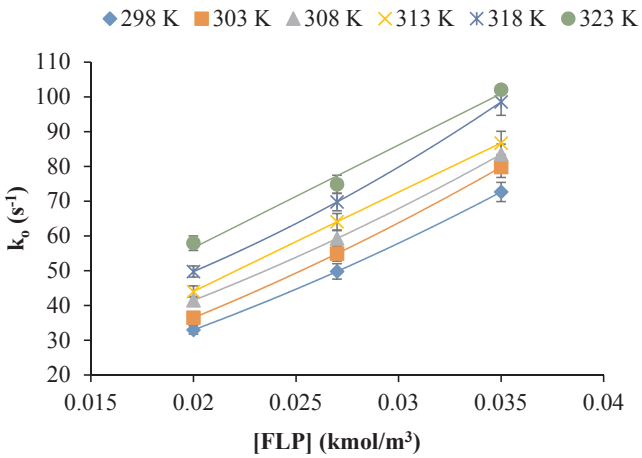

Fig. 11. Pseudo first-order rate constants as a function of FLP concentration for CO_2- AEPZ: FLP: bromobenzene system at various temperatures. All data are the average of at least eight replicate experiments, and error bars are the standard deviation of the mean.

0.02 M and 0.035 M. Experimentally obtained pseudo–first order reaction rate constants for CO_2- AEPZ: FLP: bromobenzene system at different concentrations and temperatures were given in Table 6.

The observed rate constants of the reaction between CO_2 and promoted systems with respect to FLP concentrations at various temperatures were plotted according to Eq. (2.15) as seen in Fig. 11.

Since the FLP: bromobenzene concentrations are constant in the mixture and the same temperature was used as in Section 4.1, the increase in the k_o values can be noted as the enhancing effect of the addition of AEPZ.

The forward reaction rate constants of CO_2- AEPZ: FLP: bromobenzene system were determined from the slopes of fitted lines with high regression values of $R^2 = 1$ and summarised in Table 7.

The natural logarithms of observed reaction rate constants versus FLP concentrations were plotted to determine the reaction order of the AEPZ: FLP: bromobenzene system at various temperatures as shown in Fig. 12.

The slopes of fitted to lines correspond to the reaction orders of the AEPZ: FLP: bromobenzene system which are determined to be 1.4 at

Table 7
The forward reaction rate constants of the AEPZ: FLP: bromobenzene system at various temperatures.

T (K)	k_{FLP} ($m^6/kmol^2 \cdot s$)	k ($m^3/kmol \cdot s$)
298	21,838	1256
303	24,121	1362
308	24,481	1545
313	27,618	1604
318	28,604	1853
323	–	2874

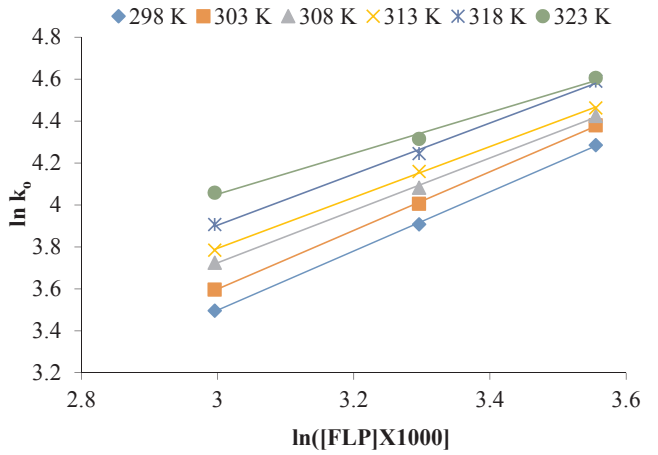

Fig. 12. Apparent reaction order plot for CO_2-AEPZ:FLP: bromobenzene system at various temperatures.

298 K; 1.4 at 303 K; 1.3 at 308 K; 1.3 at 313 K; 1.2 at 318 K; 1.0 at 323 K with regression values of $R^2 = 0.99$.

Fig. 13 shows the Arrhenius plot for 100 g/m^3 AEPZ promoted CO_2-FLP: bromobenzene system at 0.02 M, 0.027 M, and 0.035 M, respectively. Using the slopes of fitted lines, arithmetic mean activation energy for the CO_2- AEPZ: FLP: bromobenzene system was calculated as 14 kJ/mol.

4.4. The reaction kinetics of CO_2 and FLP: bromobenzene system promoted by [emim][Tf_2N]

Intrinsic reaction rates of blends of FLP: bromobenzene system with [emim][Tf_2N] were measured directly for a temperature range of 298 K–323 K. [emim][Tf_2N] concentrations were kept constant at 100 g/m^3 and the concentration of FLP: bromobenzene system were increased between 0.02 M and 0.035 M. Experimentally obtained pseudo–first order reaction rate constants for CO_2-[emim][Tf_2N]: FLP: bromobenzene system at different concentrations and temperatures were given in Table 8.

The observed rate constants of the reaction between CO_2 and promoted systems with respect to FLP concentrations at different temperatures were plotted according to Eq. (2.15) as seen in Fig. 14.

Since the FLP: bromobenzene concentrations are constant in the mixture and the same temperature was used as in Section 4.1, the increase in the k_o values can be noted as the enhancing effect of the addition of [emim][Tf_2N].

The forward reaction rate constants of CO_2-[emim][Tf_2N]: FLP: bromobenzene system were determined from the slopes of fitted lines with high regression values of $R^2 = 1$ and summarised in Table 9.

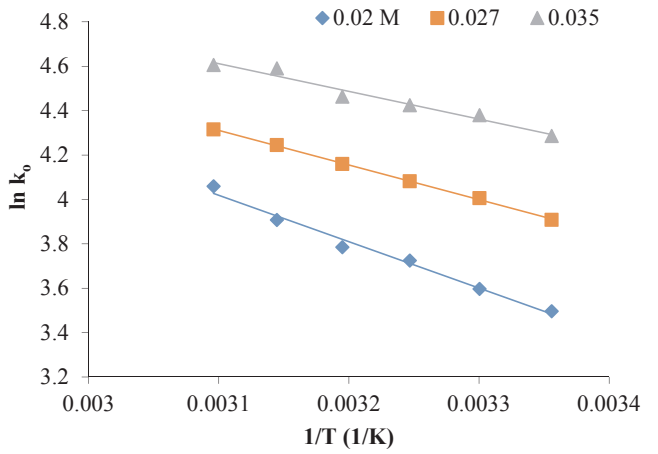

Fig. 13. Arrhenius plot for CO_2-AEPZ: FLP system in bromobenzene medium.

Table 8
Observed pseudo–first order reaction rate constants for CO_2-[emim][Tf_2N]: FLP: bromobenzene system.

	k_o (s^{-1})		
[emim][Tf_2N]: FLP: bromobenzene (kmol/m^3)	0.02	0.027	0.035
298 K	22	32	46
303 K	25	35	49
308 K	28	40	57
313 K	31	45	66
318 K	35	49	70
323 K	39	53	74

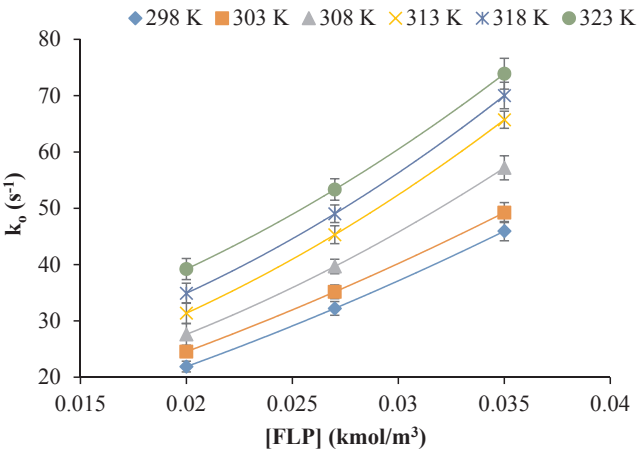

Fig. 14. Pseudo first-order rate constants as a function of FLP concentration for CO_2-[emim][Tf_2N]: FLP: bromobenzene system at various temperatures. All data are the average of at least eight replicate experiments, and error bars are the standard deviation of the mean.

Table 9
The forward reaction rate constants of the [emim][Tf_2N]: FLP: bromobenzene system at various temperatures.

T (K)	k_{FLP} (m^6/kmol^2·s)	k (m^3/kmol·s)
298	11,843	884
303	12,007	983
308	12,966	1120
313	15,103	1272
318	15,794	1421
323	16,706	1546

The natural logarithms of observed reaction rate constants versus FLP concentrations were plotted to determine the reaction order of the [emim][Tf_2N]: FLP: bromobenzene system at various temperatures as shown in Fig. 15.

The slopes of fitted to lines correspond to the reaction orders of the [emim][Tf_2N]: FLP: bromobenzene system which are determined to be 1.4 at 298 K; 1.2 at 303 K; 1.3 at 308 K; 1.3 at 313 K; 1.2 at 318 K; 1.2 at 323 K with regression values of $R^2 = 0.99$.

Fig. 16 shows the Arrhenius plot for 100 g/m^3 [emim][Tf_2N] promoted CO_2- FLP: bromobenzene system at 0.02 M, 0.027 M and 0.035 M, respectively. Using the slopes of fitted lines, arithmetic mean activation energy for the CO_2- [emim][Tf_2N]: FLP: bromobenzene system was calculated as 17 kJ/mol.

A comparison of the obtained results for FLP: bromobenzene system in the absence and presence of proposed activator for temperature range 298–313 K is summarised in Table 10.

It is seen that the proposed activators play an important role in the

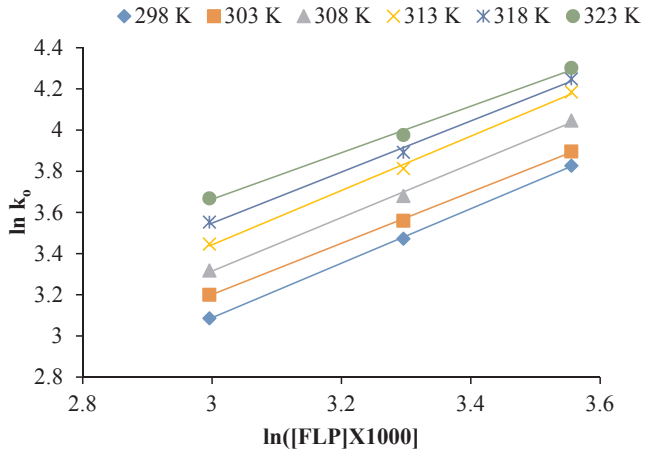

Fig. 15. Apparent reaction order plot for CO_2-[emim][Tf_2N]: FLP: bromobenzene system at various temperatures.

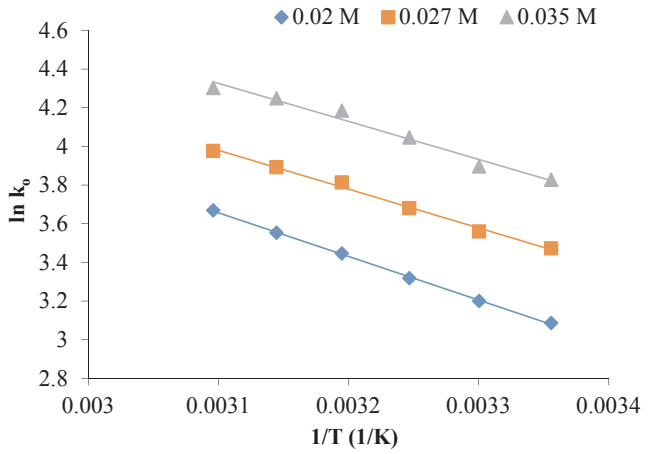

Fig. 16. Arrhenius plot for CO_2-[emim][Tf_2N]: FLP system in bromobenzene medium.

enhancement of low reaction rates of FLP: bromobenzene system. The forward reaction rate constants of promoted FLP: bromobenzene systems are comparable with some conventional aqueous amine solutions. When Table 3 is reviewed, k (m^3/kmol·s) values of promoted FLP: bromobenzene systems at the same temperature are higher than aqueous solutions of tertiary amines and some secondary amines. Furthermore, as promoted FLP: bromobenzene systems are all organic and the solvent (bromobenzene) has lower vapor pressure, lower specific heat capacity and higher boiling point than water. Due to the large specific heat capacity and vaporization enthalpy of water, the high amount of sensible heat and latent heat required for heating and vaporization of water result in high energy consumption. Non-aqueous solvent systems have shown promising prospect for less energy requirement during the regeneration, they are more preferable for post-combustion CO_2 capture than aqueous amine solutions with similar reaction rates. As a conclusion, the activator effect on reaction rates of the selected promoters can be listed as CA > AEPZ > [emim][Tf_2N] for k (m^3/kmol·s) and AEPZ > CA > [emim][Tf_2N] for k (m^6/$kmol^2$·s).

5. Conclusions

The reaction kinetics between dissolved CO_2 and FLP systems in the presence and absence of promoters, such as CA, AEPZ, [emim][Tf_2N] were examined experimentally by using stopped-flow and modelled according to a modified termolecular reaction mechanism for the first time. Based on pseudo first-order kinetics for the CO_2 absorption, the overall pseudo first-order reaction rate constants were determined from the kinetic measurements. The forward reaction rate constants and activation energies of the mentioned solvent systems were also investigated and contributed to the literature. It was observed that the low reaction rates between CO_2 and FLP system can be enhanced significantly by blending small amounts of proposed promoters. Moreover, the activation energy value of FLP: bromobenzene system (96 kJ/mol), which is quite high, decreased to 14–17 kJ/mol with the addition of the promoter. Among various amine-based solvents to be used for CO_2 capture, the selected of all organic solvents utilize the potentially lower heat requirement for regeneration as compared to aqueous solvents. To prove the accuracy of this phenomenon, further research as well as desorption kinetics, is needed to assess the applicability of this novel solvent. It is conceptually envisaged that a simple heated flash tank could replace conventional reboiler with heavy duty towards a desorberless process intensified applications by auxiliary equipment modifications. Therefore, the promoted FLP systems demonstrate that they could be promising candidates as alternatives to commonly known solvent systems for post-combustion CO_2 removal.

CRediT authorship contribution statement

Ozge Yuksel Orhan: Conceptualization, Funding acquisition, Methodology, Project administration, Supervision, Writing - original draft. **Fatima Neslisah Cihan:** Formal analysis, Investigation, Validation. **Volkan Sahin:** Investigation, Validation. **Abdulkerim Karabakan:** Methodology, Supervision. **Erdogan Alper:** Conceptualization, Methodology, Supervision.

Declaration of Competing Interest

The authors declare that they have no known competing financial interests or personal relationships that could have appeared to influence the work reported in this paper.

Acknowledgment

This work has been supported by Turkish Scientific and Technological Research Council through research grants 116M411. The authors gratefully acknowledge this support.

Table 10
Analysis summary of forward reaction rate constants for the FLP: bromobenzene-CO_2 system and promoted FLP: bromobenzene-CO_2 system at various temperatures.

Hybrid System	FLP: bromobenzene	FLP-CA: bromobenzene	FLP-AEPZ: bromobenzene	FLP-[emim][Tf_2N]: bromobenzene
k (m^3/kmol·s) (298 K)	52	937	1256	884
k (m^6/$kmol^2$·s) (298 K)	–	22,947	21,838	11,843
k (m^3/kmol·s) (303 K)	78	1152	1362	983
k (m^6/$kmol^2$·s) (303 K)	–	27,671	24,121	12,007
k (m^3/kmol·s) (308 K)	171	1352	1545	1120
k (m^6/$kmol^2$·s) (308 K)	–	28,565	24,481	12,966
k (m^3/kmol·s) (313 K)	308	1577	1604	1272
k (m^6/$kmol^2$·s) (313 K)	–	29,747	27,618	15,103

References

[1] F. Vogel, Chasing greenhouse gases at our doorstep: isotopes as a tool to identify urban carbon dioxide sources, Lc Gc N Am (2017) 12–13.
[2] E.H. Oelkers, D.R. Cole, Carbon dioxide sequestration: a solution to a global problem, Elements 4 (2008) 305–310.
[3] X.Z. Lim, How to make the most of carbon dioxide, Nature 526 (2015) 628–630.
[4] A.A. Olajire, CO2 capture and separation technologies for end-of-pipe applications - a review, Energy 35 (2010) 2610–2628.
[5] P.H.M. Feron, C.A. Hendriks, CO2 capture process principles and costs, Oil Gas Sci. Technol. 60 (2005) 451–459.
[6] R.S. Haszeldine, Carbon capture and storage: how green can black be? Science 325 (2009) 1647–1652.
[7] G.T. Rochelle, Amine scrubbing for CO2 capture, Science 325 (2009) 1652–1654.
[8] A. Wilk, L. Wieclaw-Solny, A. Tatarczuk, A. Krotki, T. Spietz, T. Chwola, Solvent selection for CO2 capture from gases with high carbon dioxide concentration, Korean J. Chem. Eng. 34 (2017) 2275–2283.
[9] D.J. Heldebrant, F. Zheng, P.K. Koech, A. Zwoster, J. Zhang, P. Humble, C. Howard, M. Elliot, C. Freeman, W. Tegrotenhuis, D. King, CO2-binding organic liquids, enhanced CO2 capture process with polarity-swing-assisted regeneration, Abstr. Pap. Am. Chem. S 243 (2012).
[10] T. Sakakura, J.C. Choi, H. Yasuda, Transformation of carbon dioxide, Chem. Rev. 107 (2007) 2365–2387.
[11] A. Benamor, N. Mahmud, M.S. Nasser, P. Tontiwachwuthikul, Reaction kinetics of carbon dioxide with 2-amino-1-butanol in aqueous solutions using a stopped-flow technique, Ind. Eng. Chem. Res. 57 (2018) 2797–2804.
[12] S.H. Zhang, Y. Shen, P.J. Shao, J.M. Chen, L.D. Wang, Kinetics, thermodynamics, and mechanism of a novel biphasic solvent for CO2 capture from flue gas, Environ. Sci. Technol. 52 (2018) 3660–3668.
[13] K. Maneeintr, R.O. Idem, P. Tontiwachwuthikul, A.G.H. Wee, Comparative mass transfer performance studies of CO2 absorption into aqueous solutions of DEAB and MEA, Ind. Eng. Chem. Res. 49 (2010) 2857–2863.
[14] B.H. Lv, K.X. Yang, X.B. Zhou, Z.M. Zhou, G.H. Jing, 2-Amino-2-methyl-1-propanol based non-aqueous absorbent for energy-efficient and non-corrosive carbon dioxide capture, Appl. Energy 264 (2020).
[15] S. Mukherjee, P. Thilagar, Frustrated Lewis pairs: design and reactivity, J. Chem. Sci. 127 (2015) 241–255.
[16] D.W. Stephan, "Frustrated Lewis pairs": a concept for new reactivity and catalysis, Org. Biomol. Chem. 6 (2008) 1535–1539.
[17] C.M. Momming, E. Otten, G. Kehr, R. Frohlich, S. Grimme, D.W. Stephan, G. Erker, Reversible metal-free carbon dioxide binding by frustrated Lewis Pairs, Angew. Chem. Int. Ed. 48 (2009) 6643–6646.
[18] D.W. Stephan, FRUSTRATED LEWIS PAIRS A metal-free landmark, Nat. Chem. 6 (2014) 952–953.
[19] D.W. Stephan, Frustrated Lewis pairs: a new strategy to small molecule activation and hydrogenation catalysis, Dalton T (2009) 3129–3136.
[20] D.W. Stephan, Activation of dihydrogen by non-metal systems, Chem. Commun. 46 (2010) 8526–8533.
[21] D.W. Stephan, G. Erker, Frustrated Lewis Pairs: metal-free hydrogen activation and more, Angew. Chem. Int. Ed. 49 (2010) 46–76.
[22] R.C. Neu, G. Menard, D.W. Stephan, Exchange chemistry of tBu(3)P(CO2)B(C6F5)(2)Cl, Dalton T 41 (2012) 9016–9018.
[23] L. Liu, B. Lukose, B. Ensing, A free energy landscape of CO2 capture by Frustrated Lewis Pairs, ACS Catal. 8 (2018) 3376–3381.
[24] S. Lindskog, The kinetic mechanisms of human carbonic Anhydrases-I and Anydrases-Ii - a computer approach, J. Mol. Catal. 23 (1984) 357–368.
[25] P. Mirjafari, K. Asghari, N. Mahinpey, Investigating the application of enzyme carbonic anhydrase for CO(2) sequestration purposes, Ind. Eng. Chem. Res. 46 (2007) 921–926.
[26] G. Sanyal, T.H. Maren, Thermodynamics of carbonic-anhydrase catalysis - a comparison between human Isoenzyme-B and Isoenzyme-C, J. Biol. Chem. 256 (1981) 608–612.
[27] G.F. Versteeg, W.P.M. Vanswaaij, On the kinetics between Co2 and alkanolamines both in aqueous and non-aqueous solutions. 1. Primary and secondary-amines, Chem. Eng. Sci. 43 (1988) 573–585.
[28] N.J.M.C. Penders-van Elk, S. Fradette, G.F. Versteeg, Effect of pKa on the kinetics of carbon dioxide absorption in aqueous alkanolamine solutions containing carbonic anhydrase at 298 K, Chem. Eng. J. 259 (2015) 682–691.
[29] N.J.M.C. Penders-van Elk, E.S. Hamborg, P.J.G. Huttenhuis, S. Fradette, J.A. Carley, G.F. Versteeg, Kinetics of absorption of carbon dioxide in aqueous amine and carbonate solutions with carbonic anhydrase, Int. J. Greenh. Gas Con. 12 (2013) 259–268.
[30] S. Kumar, M.K. Mondal, Selection of efficient absorbent for CO2 capture from gases containing low CO2, Korean J. Chem. Eng. 37 (2020) 231–239.
[31] W.C. Zheng, W.S. Jiang, R. Zhang, X. Luo, Z.W. Liang, Study of equilibrium solubility, NMR analysis, and reaction kinetics of CO2 absorption into aqueous N-1, N-2-dimethylethane-1,2-diamine solutions, Energy Fuel 34 (2020) 672–682.
[32] C.S. Ume, E. Alper, F.P. Gordesli, Kinetics of carbon dioxide reaction with aqueous mixture of piperazine and 2-amino-2-ethyl-1,3-propanediol, Int. J. Chem. Kinet. 45 (2013) 161–167.
[33] F.P. Gordesli, E. Alper, The kinetics of carbon dioxide capture by solutions of piperazine and N-methyl piperazine, Int. J. Global Warm. 3 (2011) 67–76.
[34] C.S. Ume, M.C. Ozturk, E. Alper, Kinetics of CO2 absorption by a blended aqueous amine solution, Chem. Eng. Technol. 35 (2012) 464–468.
[35] O.Y. Orhan, E. Alper, Kinetics of carbon dioxide binding by promoted organic liquids, Chem. Eng. Technol. 38 (2015) 1485–1489.
[36] J.H. Choi, Y.E. Kim, S.C. Nam, S.H. Yun, Y.I. Yoon, J.H. Lee, CO2 absorption characteristics of a piperazine derivative with primary, secondary, and tertiary amino groups, Korean J. Chem. Eng. 33 (2016) 3222–3230.
[37] A. Dey, S.K. Dash, S.C. Balchandani, B. Mandal, Investigation on the inclusion of 1-(2-aminoethyl) piperazine as a promoter on the equilibrium CO2 solubility of aqueous 2-amino-2methyl-1-propanol, J. Mol. Liq. 289 (2019).
[38] X.L. Zhao, Study on the mass-transfer performance of CO2 absorbents with a novel chemical regeneration method, Ind. Eng. Chem. Res. 54 (2015) 10983–10990.
[39] F.G. Perrin, F.D. Bobbink, E. Paunescu, Z.F. Fei, R. Scopelliti, G. Laurenczy, S. Katsyuba, P.J. Dyson, Towards a frustrated Lewis pair-ionic liquid system, Inorg. Chim. Acta 470 (2018) 270–274.
[40] Z.J. Zhao, H.F. Dong, X.P. Zhang, The research progress of CO2 capture with ionic liquids, Chinese J. Chem. Eng. 20 (2012) 120–129.
[41] M.J. Muldoon, S.N.V.K. Aki, J.L. Anderson, J.K. Dixon, J.F. Brennecke, Improving carbon dioxide solubility in ionic liquids, J. Phys. Chem. B 111 (2007) 9001–9009.
[42] O.Y. Orhan, E. Alper, Kinetics of reaction between CO2 and ionic liquid-carbon dioxide binding organic liquid hybrid systems: analysis of gas-liquid absorption and stopped flow experiments, Chem. Eng. Sci. 170 (2017) 36–47.
[43] Y. Hou, R.E. Baltus, Experimental measurement of the solubility and diffusivity of CO2 in room-temperature ionic liquids using a transient thin-liquid-film method, Ind. Eng. Chem. Res. 46 (2007) 8166–8175.
[44] P.V. Danckwerts, Reaction of Co2 with ethanolamines, Chem. Eng. Sci. 34 (1979) 443–446.
[45] J.E. Crooks, J.P. Donnellan, Kinetics and mechanism of the reaction between carbon-dioxide and amines in aqueous-solution, J. Chem. Soc. Perk T 2 (1989) 331–333.
[46] R.J. Littel, G.F. Versteeg, W.P.M. Vanswaaij, Kinetics of Co-2 with primary and secondary-amines in aqueous-solutions. 1. Zwitterion deprotonation kinetics for Dea and Dipa in aqueous blends of alkanolamines, Chem. Eng. Sci. 47 (1992) 2027–2035.
[47] M.C. Ozturk, O.Y. Orhan, E. Alper, Kinetics of carbon dioxide binding by 1,1,3,3-tetramethylguanidine in 1-hexanol, Int. J. Greenh. Gas Con. 26 (2014) 76–82.
[48] M.C. Ozturk, C.S. Ume, E. Alper, Reaction mechanism and kinetics of 1,8-diazabicyclo[5.4.0]undec-7-ene and carbon dioxide in alkanol solutions, Chem. Eng. Technol. 35 (2012) 2093–2098.
[49] M. Atakay, O. Celikbicak, B. Salih, Amine-functionalized sol-gel-based lab-in-a-pipet-tip approach for the fast enrichment and specific purification of phosphopeptides in MALDI-MS applications, Anal. Chem. 84 (2012) 2713–2720.
[50] S.H. Ali, S.Q. Merchant, M.A. Fahim, Reaction kinetics of some secondary alkanolamines with carbon dioxide in aqueous solutions by stopped flow technique, Sep. Purif. Technol. 27 (2002) 121–136.
[51] A.C. Knipe, D. Mclean, R.L. Tranter, Fast response conductivity amplifier for chemical-kinetics, J. Phys. E: Sci. Instrum. 7 (1974) 586–590.
[52] O.Y. Orhan, C.S. Ume, E. Alper, The absorption kinetics of CO2 into ionic liquid-CO2 binding organic liquid and hybrid solvents, Green Energy Technol. (2017) 241–261.
[53] O.Y. Orhan, H. Tankal, H. Kayi, E. Alper, Innovative carbon dioxide-capturing organic solvent: reaction mechanism and kinetics, Chem. Eng. Technol. 40 (2017) 737–744.
[54] M. Edali, A. Aboudheir, R. Idem, Kinetics of carbon dioxide absorption into mixed aqueous solutions of MDEA and MEA using a laminar jet apparatus and a numerically solved 2D absorption rate/kinetics model, Int. J. Greenh. Gas Con. 3 (2009) 550–560.
[55] E.B. Rinker, S.S. Ashour, O.C. Sandall, Kinetics and modeling of carbon dioxide absorption into aqueous solutions of diethanolamine, Ind. Eng. Chem. Res. 35 (1996) 1107–1114.
[56] A. Henni, J. Li, P. Tontiwachwuthikul, Reaction kinetics of CO2 in aqueous 1-amino-2-propanol, 3-amino-1-propanol, and dimethylmonoethanolamine solutions in the temperature range of 298–313 K using the stopped-flow technique, Ind. Eng. Chem. Res. 47 (2008) 2213–2220.
[57] E.B. Rinker, S.S. Ashour, O.C. Sandall, Kinetics and modeling of carbon-dioxide absorption into aqueous-solutions of N-methyldiethanolamine, Chem. Eng. Sci. 50 (1995) 755–768.
[58] H.L. Liu, T. Sema, Z.W. Liang, K.Y. Fu, R. Idem, Y.Q. Na, P. Tontiwachwuthikul, CO2 absorption kinetics of 4-diethylamine-2-butanol solvent using stopped-flow technique, Sep. Purif. Technol. 136 (2014) 81–87.
[59] T. Sema, A. Naami, Z.W. Liang, R. Idem, P. Tontiwachwuthikul, H.C. Shi, P. Wattanaphan, A. Henni, Analysis of reaction kinetics of CO2 absorption into a novel reactive 4-diethylamino-2-butanol solvent, Chem. Eng. Sci. 81 (2012) 251–259.
[60] A.K. Saha, S.S. Bandyopadhyay, A.K. Biswas, Kinetics of Absorption of Co2 into aqueous-solutions of 2-amino-2-methyl-1-propanol, Chem. Eng. Sci. 50 (1995) 3587–3598.
[61] P.W.J. Derks, T. Kleingeld, C. van Aken, J.A. Hogendoom, G.F. Versteeg, Kinetics of absorption of carbon dioxide in aqueous piperazine solutions, Chem. Eng. Sci. 61 (2006) 6837–6854.